Crack Front Propagation and Fracture in a Graphite Sheet: A Molecular-Dynamics Study on Parallel Computers

Andrey Omeltchenko, Jin Yu, Rajiv K. Kalia, and Priya Vashishta

Concurrent Computing Laboratory for Materials Simulations, Department of Physics and Astronomy and Department of Computer Science, Louisiana State University, Baton Rouge, Louisiana 70803

(Received 29 October 1996)

Crack propagation in a graphite sheet is investigated with million atom molecular-dynamics simulations based on Brenner's reactive empirical bond-order potential. For certain crystalline orientations, multiple crack branches with nearly equal spacing sprout as the crack tip reaches a critical speed of $0.6V_R$, where V_R is the Rayleigh wave speed. This results in a fracture surface with secondary branches and overhangs. Within the same branch the crack-front profile is characterized by a roughness exponent, $\alpha = 0.41 \pm 0.05$. However, for interbranch fracture surface profiles the return probability yields $\alpha = 0.71 \pm 0.10$. Fracture toughness is estimated from Griffith analysis and local-stress distributions. [S0031-9007(97)02755-5]

PACS numbers: 62.20.Mk, 61.20.Ja, 61.43.Hv, 81.40.Np

Instabilities in crack-front propagation have been the focus of many recent experimental [1,3], theoretical [4–6], and numerical studies [6,7]. Experimental investigations of fracture dynamics in brittle materials have revealed that the flow of energy into a system increases the crack-front speed until it reaches a critical value, V_c, where local crack branches sprout to facilitate the dissipation of energy. The experimental value of V_c is found to be $0.36V_R$, where V_R is the Rayleigh wave speed in the material [1]. Marder and Liu [6] have investigated this issue in a model 2D system of coupled springs which snap beyond a critical displacement to mimic brittle behavior. In this model system, local crack branches appear when the crack-front speed exceeds $0.66V_R$. Back in 1951 Yoffe [8] had found from linear elasticity that straight-line crack-front propagation in a nondissipative 2D system was unstable at crack-front speeds above $0.6V_R$.

There is an alternative scenario of energy dissipation during crack-front propagation [9]. Experimental studies indicate that stress fields around the crack front cause the growth and coalescence of preexisting microvoids in the path of the crack front. Recent molecular-dynamics (MD) simulation studies [10] of fracture in amorphous silicon nitride also find that an increase in the external strain causes micropores to grow and coalesce into larger entities until one of the pores percolates through the entire system.

Another aspect that has drawn a great deal of attention in recent years is the morphology of fracture surfaces. The pioneering work of Mandelbrot *et al.* [11] and many subsequent experimental studies have established that rough fracture surfaces are self-affine objects with a typical roughness exponent of 0.8 for 3D and 0.7 for 2D fracture. Careful experimental studies [12–14] indicate that for rapidly moving crack fronts or above a certain crossover length these roughness exponents do not depend on material characteristics. However, a smaller value of the roughness exponent (close to 0.5) is found on nanometer length scales or in the case of slow crack propagation [14,15]. The crossover between these two different regimes of fracture has been observed in experiments on Ti_3Al-based alloys [14] and MD simulations of silicon nitride [10]. Recently, self-affine behavior has been observed in branched cracks, and their roughness exponents are consistent with the universal values [13].

The purpose of this Letter is to describe the results of a MD simulation dealing with morphological and dynamic aspects of fracture in a real brittle system, namely, a single graphite sheet (graphine). Molecular dynamics simulations on a 1.1×10^6 particle graphite system show multiple crack branches sprouting off the primary crack front when its speed exceeds $0.6V_R$. The spacing between adjacent local crack branches is nearly constant, and the number of branches grows with time as more energy flows into the system. Most of the local crack branches die after propagating for a short while. Fracture profiles of individual branches have a roughness exponent of 0.4, whereas the return probability for interbranch fracture profiles yields a roughness exponent of 0.7.

Our molecular-dynamics simulations are based on reactive bond order potentials for hydrocarbons developed by Brenner *et al.* [16] In this model, the potential energy is written as

$$E_b = \sum_i^N \sum_{j>i}^N [\phi_{ij}^R(r_{ij}) - b_{ij}\phi_{ij}^A(r_{ij})], \qquad (1)$$

where $\phi^R(r)$ is the repulsive part of the potential and $\phi^A(r)$ is an attractive pair potential which represents the chemical bonding between atoms i and j. The attractive part is modified by a bond-order term, b_{ij}, which accounts for different strengths of single, double, and triple bonds. The bond order depends on local coordination and bond angles. Additional terms are included in b_{ij} to describe bonds which are part of a conjugated system or have

 0031-9007/97/78(11)/2148(4)$10.00

radical character as well as the energetics of rotation around dihedral angles for carbon-carbon double bonds. The parameters of the model have been fitted to an extensive database of experimental values and *ab initio* calculations. This potential has been successfully used to investigate various carbon and hydrocarbon systems [17].

Dynamic fracture is studied in a single 1500 Å $\times$ 2000 Å graphite sheet containing 1.1×10^6 atoms. (Dangling bonds at the boundaries are terminated with hydrogen atoms.) The simulations are run with a time step of 1 fs at 300 K. While the initial configuration is completely two dimensional, the dynamics of atoms is followed in three dimensions. Fracture in the graphite sheet is studied under constant applied strain after inserting a small triangular notch of length 30 Å. The morphology of fracture surfaces and crack-front dynamics is analyzed by converting atomic configurations into two-dimensional images with pixel size of 3 Å. Roughness exponents are calculated from the height-height correlation function and, alternatively, from return probability histograms of fracture surfaces [13]. The crack-front dynamics is determined from snapshots of the system taken every 0.05 ps.

We consider two possible orientations of the graphite sheet with respect to the applied strain. The geometry in which the applied strain is parallel to some of the covalent bonds [Fig. 1(a)] is referred to as $G(1,1)$. However, when some of the bonds are perpendicular to the direction of the applied strain [Fig. 1(b)], we call this orientation $G(1,0)$. In both cases, after applying a given strain we insert a notch and then monitor the behavior of the system, keeping the external strain fixed. Two million-particle simulations are performed for the $G(1,0)$ configuration at external strains of 12% and 16% [18].

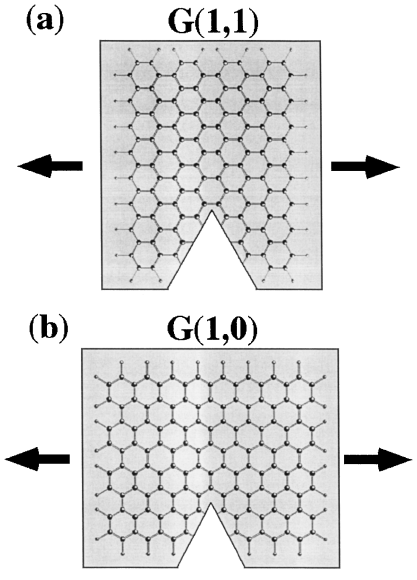

FIG. 1. Orientations in fracture simulations of the graphite sheet: In $G(1,1)$ orientation the applied strain is parallel to some of the C-C bonds and in the $G(1,0)$ orientation the strain is perpendicular to some of the bonds.

For both $G(1,1)$ and $G(1,0)$ orientations, the initial notch of length 30 Å does not propagate for applied strains less than 12%. In the case of $G(1,1)$, the notch inserted in the graphite sheet under 12% strain propagates at an average speed of 6.2 km/s. This is 50% of the calculated Rayleigh wave speed for the graphite sheet. It is evident in the inset in Fig. 2 that the graphite sheet in the $G(1,1)$ orientation undergoes cleavage fracture.

We have also estimated the fracture toughness of the graphite sheet in the $G(1,1)$ orientation using the MD approach. The system with a notch of 50 Å has been subjected to different strains. Applying the Griffith criterion with the surface energy determined from the final fracture surface, the critical stress is estimated to be 71 GPa [19]. The crack starts propagating at a stress of 66 GPa, which corresponds to a critical strain of 10%. From these results, the value of the fracture toughness (defined as $\sigma_F\sqrt{c}$, where σ_F is the critical stress at which the crack starts propagating, and c is the length of the notch) is found to be 4.7 MPa m$^{1/2}$. We have also calculated the local-stress distribution around the notch just before the onset of crack propagation. The data are well described by $1/\sqrt{r}$ dependence with a stress intensity factor of 6 MPa m$^{1/2}$. The angular dependence of the local stresses is also in good agreement with the predictions of the elasticity theory.

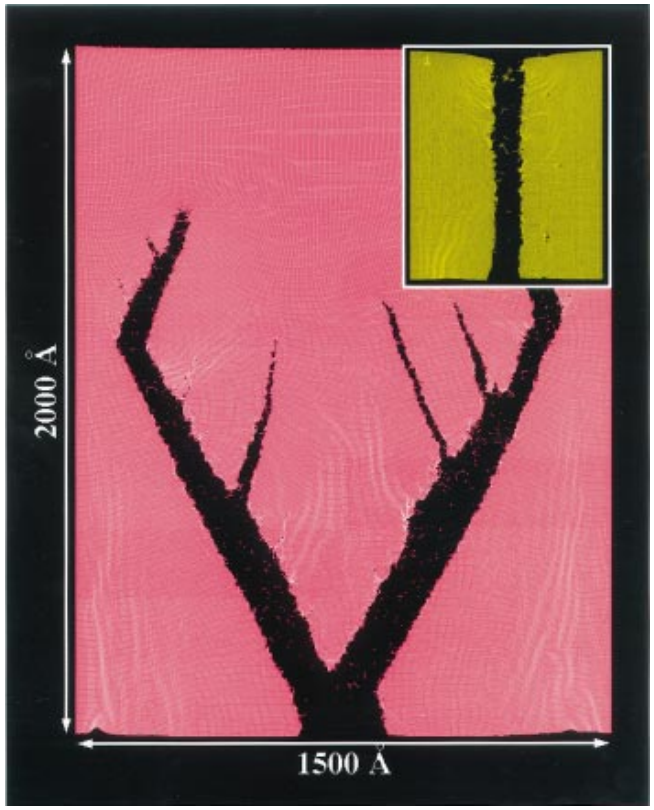

FIG. 2(color). Branched crack in a graphite sheet with $G(1,0)$ orientation and 12% strain. Inset: cleavage fracture for $G(1,1)$ orientation.

Figure 2 shows that fracture in the $G(1,0)$ orientation is quite different from that observed in the case of $G(1,1)$. After propagating for 2 ps, the crack front splits up into two nearly symmetric branches, oriented 30° relative to the primary crack front. Each branch now propagates in the same crystallographic direction as in the case of $G(1,1)$ and quickly accelerates to the same terminal speed of 6.2 km/s. Subsequently they give rise to more branches, which are oriented 60° relative to the "mother" branches. Most of the "daughter" branches propagates for less than 10 ps and then their motion completely subsides. In contrast, the mother branches continue to propagate maintaining the same speed until the sample completely fractures. After 18 ps, the mother branches are reflected by the boundaries. Although crack branching increases the amount of energy dissipated due to surface creation, we do not find any significant differences in the critical stress from that in the case of $G(1,1)$.

Figure 3 shows various crack branches in the $G(1,0)$ orientation of the graphite sheet after it fractures under an applied strain of 16%. In this case also, the notch almost immediately splits up into two secondary branches which give rise to almost equally spaced local branches (the spacing is ~200 Å). The branching occurs more frequently than in the previous case (12% strain) and, in addition, the fracture surface contains much smaller branches with a spacing of ~50 Å.

FIG. 3(color). Fracture in a graphite sheet subjected to 16% strain in the $G(1,0)$ orientation.

Crack tip positions (X and Y) determined from snapshots of the crack are plotted in the inset of Fig. 4. For a branched crack, multiple crack tips corresponding to different branches are shown so that the crack-tip trajectories directly correspond to the final shape of the crack (compare Fig. 3 and the inset in Fig. 4). Figure 4 also shows the time evolution of various local crack branches. It is evident that they all maintain nearly the same velocity until some of them slow down and stop. The speed along the direction of propagation is found to be 7.2 km/s—nearly two-thirds of the Rayleigh wave speed. Most of the local branches have a lifetime of <5 ps; however, a few local branches survive much longer and one of them, in particular, has a sufficiently long lifetime of 20 ps.

We have also examined the morphology of fracture surfaces by calculating their roughness exponents. For branched cracks, the roughness exponent is calculated from the return probability $P(z,r)$, where r denotes the coordinates parallel to the fracture surface and z is measured perpendicular to the surface. $P(z,r)$, the probability that the point $(r_0 + r, z_0 + z)$ belongs to the fracture surface given that (r_0, z_0) is on the surface, scales as $P(z,r) \sim r^{-\alpha}$, where α is the roughness exponent. In the absence of branching, the roughness exponents may be calculated from the height-height correlation function,

$$[g(r)]^2 = \langle h(r)h(0)\rangle\,, \tag{2}$$

where r is measured along the direction of crack propagation, h is the height perpendicular to the fracture surface, and the average is taken over the whole surface. For self-affine surfaces, $g(r)$ scales as r^{α}. For branched cracks, the average in Eq. (2) is restricted to correlations within the same branch. Figure 5(a) shows $g(r)$ calculated for a long single branch in the graphite sheet under 16% strain in the $G(1,0)$ orientation. From these data, we find the "intrabranch" roughness exponent $\alpha = 0.41 \pm 0.05$.

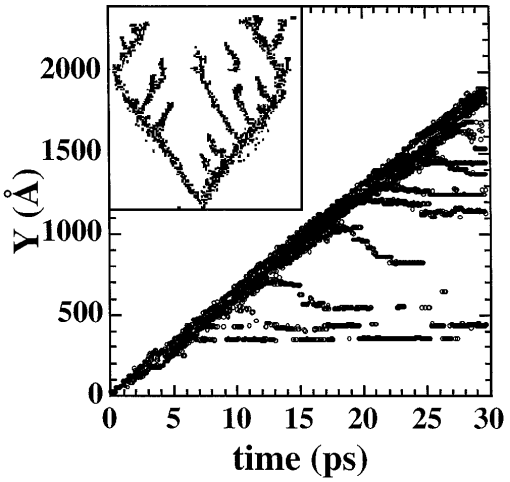

FIG. 4. Crack-tip positions along the Y axis as a function of time; the geometry is $G(1,0)$ and the applied strain is 16%. The inset is a cumulative plot of all the crack-tip positions in the XY plane recorded every 0.05 ps.

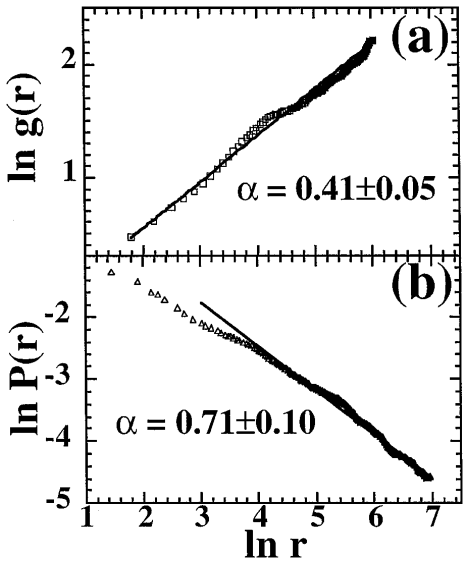

FIG. 5. Roughness exponents for the fracture profile shown in Fig. 2. These exponents are determined from: (a) the height-height correlation function; and (b) the return probability histogram.

For the same fracture surface, we have also calculated the return probability histogram $P(x, y)$. In this case, the average is taken over the whole fracture surface, and the correlations are no longer restricted to the same branch. The return probability along the direction of the branches (30° with respect to the Y axis) is plotted in Fig. 5(b). Above the crossover length of about 50 Å, the data in Fig. 5(b) can be fitted to $P(z, r) \sim r^{-\alpha}$ with $\alpha = 0.71 \pm 0.10$. This value of the roughness exponent corresponds to "interbranch" correlations, which are dominant above the crossover length. Below the crossover length, the scaling in Fig. 5(b) is consistent with the intrabranch roughness exponent $\alpha \approx 0.4$, calculated from the height-height correlation function. Similar scaling behavior is also observed for the $G(1, 0)$ orientation with 12% strain; the only difference is that the crossover length is 150 Å because of larger spacing between branches. Because our MD simulations involve large stresses and fast crack propagation, our values for the crossover length are much smaller than typical experimental values [14] (few microns).

In conclusion, large-scale molecular-dynamics calculations based on a reactive bond-order potential reveal that for a certain orientation of the graphite sheet, where some of the C-C bonds are parallel to the applied strain, the system undergoes cleavage fracture. In the perpendicular orientation, we find multiple crack branches sprouting off the primary crack front at regular intervals. These branches appear at a critical crack-tip speed [(50–60)% of the Rayleigh wave speed depending on the applied strain]. The morphology of crack branches is well characterized by two values of the roughness exponent α: Below a certain crossover length and within the same local branch, $\alpha \approx 0.4$; for interbranch correlations exceeding the crossover length, $\alpha \approx 0.7$. Fracture toughness is estimated to be 4.7 MPa $m^{1/2}$ from Griffith analysis. This is consistent with the stress intensity factor ($\sim$6 MPa $m^{1/2}$) extracted from the local-stress distribution.

We would like to thank Dr. Brenner for providing us with the latest version of his interatomic potentials for hydrocarbons. This work was supported by DOE, NSF, AFOSR, USC-LSU Multidisciplinary University Research Initiative, Army Research Office, and Louisiana Education Quality Support Fund (LEQSF). Simulations were performed on the parallel machines in the Concurrent Computing Laboratory for Materials Simulations (CCLMS) at Louisiana State University. The facilities in the CCLMS were acquired with equipment enhancement grants awarded by LEQSF.

[1] E. Sharon, S. P. Gross, and J. Fineberg, Phys. Rev. Lett. **74**, 5096 (1995); Phys. Rev. Lett. **76**, 2117 (1996).
[2] S. P. Gross *et al.*, Phys. Rev. Lett. **71**, 3162 (1993).
[3] J. Fineberg *et al.*, Phys. Rev. Lett. **67**, 457 (1991); Phys. Rev. B **45**, 5146 (1992).
[4] J. S. Langer, Phys. Rev. A **46**, 3123 (1992).
[5] K. Runde, Phys. Rev. E **49**, 2597 (1994).
[6] M. Marder and X. Liu, Phys. Rev. Lett. **71**, 2417 (1993).
[7] F. F. Abraham *et al.*, Phys. Rev. Lett. **73**, 272 (1994).
[8] E. Yoffe, Philos. Mag. **42**, 739 (1951).
[9] K. Ravi-Chadar and W. G. Knauss, Int. J. Fract. **26**, 141 (1984).
[10] A. Nakano, R. K. Kalia, and P. Vashishta, Phys. Rev. Lett. **75**, 3138 (1995).
[11] B. B. Mandelbrot, D. E. Passoja, and A. J. Paullay, Nature (London) **308**, 721 (1984).
[12] K. J. Måløy, A. Hansen, E. L. Hinrichsen, and S. Roux, Phys. Rev. Lett. **68**, 213 (1992); T. Engoy, K. J. Måløy, A. Hansen, and S. Roux, Phys. Rev. Lett. **73**, 834 (1994).
[13] E. Bouchaud, G. Lapasset, and J. Planès, Europhys. Lett. **13**, 73 (1990); E. Bouchaud, G. Lapasset, J. Planès, and S. Navéos, Phys. Rev. B **48**, 2917 (1993).
[14] E. Bouchaud and S. Navéos (to be published).
[15] V. Y. Milman, R. Blumenfeld, N. A. Stelmachenko, and R. C. Ball, Phys. Rev. Lett. **71**, 204 (1993); V. Y. Milman, N. A. Stelmachenko, and R. Blumenfeld, Prog. Mater. Sci. **38**, 425 (1994).
[16] D. W. Brenner, Phys. Rev. B **42**, 9458 (1990); D. W. Brenner and S. B. Sinnott (to be published).
[17] S. Sinnott, R. J. Colton, C. T. White, and D. W. Brenner, Surf. Sci. Lett. **316**, L1055 (1994); J. A. Harrison and D. W. Brenner, J. Am. Chem. Soc. **116**, 10 399 (1994); B. J. Garrison, E. J. Dawnkaski, D. Srivastava, and D. W. Brenner, Science **255**, 835 (1992); D. H. Robertson, D. W. Brenner, and C. T. White, J. Phys. Chem. **96**, 6133 (1992).
[18] Smaller simulations involving 10^5 atoms (450 Å × 600 Å graphite sheet) have also been performed to cover a much broader range of parameters.
[19] For a two-dimensional system, stresses should be measured in units of N/m instead of Pa (N/m^2). However, in order to make connection with the three-dimensional system we divide the result by the spacing between graphite layers (3.4 Å).